

Temperature fields in sliding solids with internal heat sources

W. Y. D. YUEN

Research and Technology Centre, Sheet & Coil Products Division, BHP Steel, P.O. Box 77,
 Port Kembla, NSW 2505, Australia

(Received 21 September 1992 and in final form 12 March 1993)

Abstract—This paper examines the heat transfer between two sliding solids in contact over a fixed region with internal heat sources generated in the solids. Asymptotic solutions for the heat flux distribution along the contact and temperature fields in the solids are derived for large Peclet numbers. Comparisons with numerical solutions indicate that the asymptotic analysis is valid for Peclet numbers higher than 10. Simplified expressions which are suitable for practical engineering applications, for the temperature distribution beyond the contact and the characterization of the thermal penetration into the solids, are also derived.

1. INTRODUCTION

THE CONDUCTION of heat between bodies in perfect contact has been extensively studied since it finds applications in many industrial processes, and forms a building block for the examination of thermal systems with imperfect contacts. Schneider *et al.* [1] and Sadhal [2, 3] studied the steady-state and transient thermal variations in stationary solids which were in contact over a finite region. Jaeger [4] discussed the Green's functions for the transient and steady-state temperature fields in a stationary semi-infinite solid with heat sources moving at a constant speed on the surface of the solid. This formulation provided a basis for numerical studies of heat transfer between two moving bodies. The resultant temperature fields in them were later studied by Allen [5], Cameron *et al.* [6] and Symm [7] and, more recently, by Blahey and Schneider [8].

In the context of strip rolling, Yuen has recently derived asymptotic solutions for the heat transfer between two moving semi-infinite solids in contact over a finite fixed region. Both the heat partition to each body and the resultant temperature fields have been examined [9–11]. The cases where the bulk temperatures of the solids are different [9, 10] and where heat energy is generated along the contact region [11] have been considered separately. In strip rolling, the former relates to the hot rolling condition for which the rolls and the workpiece have very different temperatures, and the latter relates to the frictional energy generated along the contact region due to the rolls and the workpiece moving at different speeds. Yet another area of interest involves heat energy being generated in one or both solids within the contact region, which is the subject of investigation in this paper. This heat energy is caused, in strip rolling, by the plastic deformation in the workpiece and the elastic hysteresis in the rolls; while in other applications, it could be induced by internal heat sources such as induction heating.

2. MATHEMATICAL FORMULATION

Consider two semi-infinite solids moving in the same direction and being in perfect contact over a finite region. It is assumed that the solid surfaces are perfectly insulated outside the contact region, as illustrated in Fig. 1. Consider further that heat energy is generated in one of the solids, say, body 2, within the contact region. This paper examines the two-dimensional steady-state behaviour of such a thermal system. The situation where heat source is present in body 1 or in both bodies is a trivial extension of the solutions derived in this paper and will not be elaborated here.

Based on a Green's function formulation, the temperature change in body *i*, $T_i(x, y)$, due to the heat flux across the contact region is given by [4, 9]

$$T_i(x, y) = \mp \frac{1}{\pi} \int_0^1 \frac{\partial T_i}{\partial y}(x', 0) e^{p(x-x')} \times K_0\{P_i[(x-x')^2 + y^2]^{1/2}\} dx' \quad (1)$$

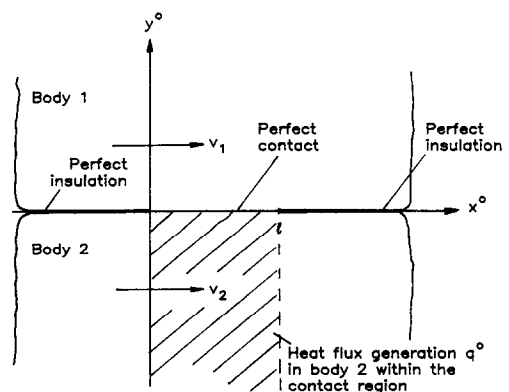


FIG. 1. Thermal system under study: two moving bodies in contact over a fixed region.

NOMENCLATURE

A	form factor	$T(x, y)$	temperature change (from the bulk temperature of the body prior to contact)
$f(x)$	$\partial T_1 / \partial y _{y=0}$	T_0	bulk temperature difference between body 2 and body 1
$f_0(x), f_1(x)$	terms defined in equation (14)	$T_d(x, y)$	temperature change (from the bulk temperature of the body prior to contact) due to the internal heat source in the body
$I_a, I_b, I_c, I_{c1}, I_{c2}$	integrals defined in equations (A.1), (B.1), (C.1), (C.3) and (C.5), respectively	T_{ip}	maximum temperature change in body i
I_A, I_B	integrals defined in equations (26) and (28), respectively	$T_m(y)$	maximum temperature change reached at a depth y (non-dimensionalized) below the body surface
$I_i[f(x)]$	integral defined in equation (10)	T_p	maximum temperature change in the body
J_v	integral defined in equation (A.5)	v_i	speed of body i
k	thermal conductivity	(x, y)	Cartesian coordinate pair, non-dimensionalized with the contact length, l
k_r	ratio of the thermal conductivity of body 2 to that of body 1	(x^0, y^0)	Cartesian coordinate pair
l	contact length	x_m	x -coordinate at which $T_m(y)$ is reached.
p	scalar defined in equation (B.1)		
P	Peclet number, $vl/(2\alpha)$		
P_r	ratio of the Peclet number of body 2 to that of body 1		
$q(x, y)$	non-dimensionalized rate of internal heat generation per unit volume		
$q^0(x^0, y^0)$	rate of internal heat generation per unit volume		
q_0	non-dimensionalized rate of (uniform) internal heat generation per unit volume		
q_{av}^0	average heat flux distribution (per unit area) over the contact region		
$(q_{av}^0)_1, (q_{av}^0)_2, (q_{av}^0)_3$	average heat flux distribution (per unit area) over the contact for the friction effect, bulk temperature difference effect and deformation effect, respectively		
q_d^0	rate of deformation heat generated per unit volume under the contact region for body 2		
q_f^0	rate of frictional heat generated per unit area along the contact region		
S_1, \dots, S_5	series defined in equations (41)–(44), and (47), respectively		
		Greek symbols	
		α	thermal diffusivity
		β_0, β_1	terms defined in equations (17) and (22)
		$\varepsilon_1, \varepsilon_2$	small terms defined in Section 3.1
		η_i	$P_i y^2 / 2$
		ν	factor defined in equation (A.2)
		$\xi_1, \xi'_1, \xi_2, \xi'_2$	terms defined after equation (31)
		(ρ, θ)	cylindrical coordinate pair defined after equation (34).
		Subscripts (unless defined above)	
		1	body 1
		2	body 2
		i	body i .

where

$$P_i = \frac{1}{2} v_i l / \alpha_i, \quad x = x^0 / l, \quad \text{and} \quad y = y^0 / l.$$

Here, subscript $i = 1, 2$ and the upper and lower signs in equation (1) refer to bodies 1 and 2, respectively; (x^0, y^0) are the Cartesian coordinates with the origin located at the leading edge of the contact as shown in Fig. 1; l is the contact length; $T_i(x, y)$ the temperature change of body i at the non-dimensionalized coordinates (x, y) due to the heat flux at the contact region; v_i the speed of body i (moving in the x^0 direction); α_i and P_i are the thermal diffusivity and Peclet number of body i , respectively; and $K_0(\)$ is the modified Bessel function of the second kind.

The overall temperature change of body 1 is given

by $T_1(x, y)$ while that for body 2 is given by the sum of $T_2(x, y)$ and $T_d(x, y)$, the latter of which is contributed from the internal heat generation in body 2 and can be deduced by integrating the Green's function of a moving line source in an infinite medium [12]

$$T_d(x, y) = \frac{P_2}{\pi} \int_0^1 \int_{-\infty}^{\infty} q(x', y') e^{P_2(x-x')} \times K_0 \{ P_2 [(x-x')^2 + (y-y')^2]^{1/2} \} dy' dx' \quad (2)$$

where

$$q(x, y) = \frac{l \alpha_2 q^0(x^0, y^0)}{k_2 v_2}. \quad (3)$$

Here, $q^0(x^0, y^0)$ is the rate of internal heat generation

per unit volume at (x^0, y^0) and k_i the thermal conductivity of body i . Since a semi-infinite body with insulated surface is being considered here for the T_d effect (for body 2), equation (2) may be integrated by forcing the internal heat flux term to be symmetrical about the x -axis, namely, $q(x, y) = q(x, -y)$.

The boundary conditions for (i) an initially equal and uniform bulk temperature of the bodies prior to contact, (ii) insulated surfaces outside the contact region, (iii) continuity of temperatures at the contact region (perfect contact assumed) and (iv) conservation of heat fluxes at the contact region are, respectively,

$$T_1(-\infty, y) = T_2(-\infty, y) + T_d(-\infty, y) = 0 \quad (4)$$

$$\frac{\partial T_1}{\partial y}(x, 0) = \frac{\partial T_2}{\partial y}(x, 0) + \frac{\partial T_d}{\partial y}(x, 0) = 0$$

$$\text{for } x < 0 \text{ and } x > 1 \quad (5)$$

$$T_1(x, 0) - [T_2(x, 0) + T_d(x, 0)] = 0 \quad \text{for } 0 < x < 1 \quad (6)$$

$$-\frac{\partial T_1}{\partial y}(x, 0) + k_r \left[\frac{\partial T_2}{\partial y}(x, 0) + \frac{\partial T_d}{\partial y}(x, 0) \right] = 0$$

$$\text{for } 0 < x < 1 \quad (7)$$

where

$$k_r = \frac{k_2}{k_1}. \quad (8)$$

It is noted that equations (4) and (5) are satisfied implicitly because of a proper choice of the Green's functions in equations (1) and (2). From equations (6) and (7), with equation (1) and noting that $\partial T_d / \partial y|_{y=0} \equiv 0$, a Fredholm integral equation of the first kind in the unknown $\partial T_1 / \partial y|_{y=0}$ is obtained

$$I_1[f(x)] + \frac{1}{k_r} I_2[f(x)] = -\pi T_d(x, 0)$$

$$\text{for } 0 < x < 1 \quad (9)$$

where

$$I_i[f(x)] = \int_0^1 f(x') e^{P_i(x-x')} K_0(P_i|x-x'|) dx' \quad (10)$$

and

$$f(x) = \frac{\partial T_1}{\partial y}(x, 0). \quad (11)$$

Thus, the heat flux distribution to body 1 at the contact region can be found by solving equation (9) and the resultant temperature fields in both bodies obtained from equations (1) and (2). An asymptotic solution for the heat flux distribution across the contact region, which applies when the Peclet numbers (P_1 and P_2) are large, is derived below. (In strip rolling, the Peclet numbers are over 4000.) This is followed by a discussion of the temperature fields in the bodies.

3. ASYMPTOTIC SOLUTIONS

To proceed further, a uniformly distributed heat source is considered, namely

$$q(x, y) \equiv \begin{cases} q_0 & \text{for } 0 < x < 1 \\ 0 & \text{for } x < 0 \text{ and } x > 1. \end{cases} \quad (12)$$

Thus, the integrals in equation (2) may be performed, giving

$$T_d(x, y) = \begin{cases} \frac{1}{2} q_0 e^{2P_2 x} \left(\frac{1 - \exp(-2P_2)}{P_2} \right) & \text{for } x < 0 \\ q_0 \left\{ x + \frac{1 - \exp[-2P_2(1-x)]}{2P_2} \right\} & \text{for } 0 < x < 1 \\ q_0 & \text{for } x > 1. \end{cases} \quad (13)$$

3.1. Heat flux at the contact region

Following Yuen's approach [9], consider the region 'away' from the leading and trailing edges of the contact such that $\varepsilon_1 < x < (1 - \varepsilon_2)$, where $0 < \varepsilon_1, \varepsilon_2 \ll 1$ but $P_i \varepsilon_1$ and $P_i \varepsilon_2 \gg 1$ ($i = 1, 2$). It can be shown, with $f(x)$ written as

$$f(x) = f_0(x) + f_1(x) + f_2(x) + \dots \quad (14)$$

where

$$f_i(x) = O[f_{i-1}(x)] \quad \text{for } i = 1, 2, 3, \dots \quad (15)$$

that the leading order term $f_0(x)$ may be determined by solving the integral equation

$$\int_0^x \frac{f_0(x-u)}{u^{1/2}} du = \frac{1}{2} \pi \beta_0 x \quad (16)$$

where

$$\beta_0 = -2 \left(\frac{2P_2}{\pi} \right)^{1/2} \left(\frac{k_r}{1 + k_r P_r^{1/2}} \right) q_0 \quad (17)$$

and

$$P_r = \frac{P_2}{P_1}. \quad (18)$$

The solution of equation (16) is straight-forward, giving

$$f_0(x) = \beta_0 x^{1/2}. \quad (19)$$

The integral equation for the next order term, $f_1(x)$, may be obtained by substituting equation (19) into equation (9), and making use of the identity (derived in Appendix A)

$$\int_0^1 (1-u)^{1/2} e^{Pu} K_0(Pu) du + \int_0^\infty (1+u)^{1/2} e^{-Pu} K_0(Pu) du = \left(\frac{\pi}{2P} \right)^{3/2} (4+P). \quad (20)$$

It can be shown, after dropping smaller order terms, that

$$I_1[f_1(x)] + \frac{1}{k_r} I_2[f_1(x)] = \frac{\pi^{3/2}}{(2P_2)^{1/2}} \left\{ \frac{1+k_r P_r^{1/2}}{k_r} \right\} \beta_1$$

for $0 < x < 1$ (21)

where

$$\beta_1 = - \frac{q_0}{(2\pi P_2)^{1/2}} \left\{ \frac{k_r}{1+k_r P_r^{1/2}} \right\} \left\{ 1 - \frac{1+k_r P_r^{3/2}}{2(1+k_r P_r^{1/2})} \right\}$$

(22)

Equation (21) has the same form as equation (9). Following the same procedure and making use of the results of Yuen [9], the solution for $f_1(x)$ is

$$f_1(x) = \frac{\beta_1}{x^{1/2}}$$

(23)

Hence, to the leading orders, we obtain the heat flux distribution to body 1 at the contact region

$$f(x) \approx \beta_0 x^{1/2} + \frac{\beta_1}{x^{1/2}}$$

(24)

3.2. Surface temperatures

Further approximations to the integral of equation (1) need to be made to obtain the entire temperature fields of the bodies; these will be discussed in Section 3.3. However, the surface temperatures, which are of interest in most practical applications, can be derived readily as follows. From equation (1), the surface temperature of body i is given by

$$T_i(x, 0) = \mp \frac{1}{\pi} \int_0^1 \frac{\partial T_i}{\partial y}(x', 0) e^{\rho_i(\alpha-x')} \times K_0(P_i|x-x'|) dx'$$

(25)

requires the results of the following integrals:

$$I_A = \int_1^\infty (u-1)^{-1/2} e^{-Pu} K_0(Pu) du$$

(26)

$$= \pi \left(\frac{\pi}{2P} \right)^{1/2} \operatorname{erfc}(2P)^{1/2}$$

(27)

and

$$I_B = \int_1^\infty (u-1)^{1/2} e^{-Pu} K_0(Pu) du$$

(28)

$$= \frac{\pi}{2} (2P)^{-5/4} e^{-P} W_{-3/4, -3/4}(2P)$$

(29)

$$= \frac{1}{2} \left(\frac{\pi}{2P} \right)^{3/2} (\frac{1}{2} - 2P) \operatorname{erfc}(2P)^{1/2} + \frac{\pi}{4P} e^{-2P}$$

(30)

where $W_{a,b}(\cdot)$ and $\operatorname{erfc}(\cdot)$ are the Whittaker and complementary error functions, respectively. The result of I_A follows from Appendix C of ref. [9], the intermediate result of I_B (equation (29)) may be obtained from ref. [13] and the final result (equation (30)) from the properties of the Whittaker function (e.g. see ref. [14]). For the region $0 < x < 1$, the identity of equation (20) is again made use of; and for the region $x > 1$, the leading order term can be derived by expanding the modified Bessel function asymptotically for large argument. After some mathematical manipulations, the final results for the surface temperatures of the bodies are

$$T_i(x, 0) = \begin{cases} \xi_i \left[\frac{\pi^{1/2}}{(2P_i)^{3/2}} (4 - P_i|x|) \operatorname{erfc}(2P_i|x|)^{1/2} + \frac{|x|^{1/2}}{4P_i} e^{-2P_i|x|} \right] + \xi'_i \left(\frac{\pi}{2P_i} \right)^{1/2} \operatorname{erfc}(2P_i|x|)^{1/2} & \text{for } x < 0 \\ \xi_i \frac{\pi^{1/2}}{(2P_i)^{3/2}} (4 + P_i x) + \xi'_i \left(\frac{\pi}{2P_i} \right)^{1/2} & \text{for } 0 < x < 1 \\ \xi_i \frac{x}{(2\pi P_i)^{1/2}} \left[\tan^{-1}(x-1)^{-1/2} - \frac{(x-1)^{1/2}}{x} \right] + \xi'_i \left(\frac{2}{\pi P_i} \right)^{1/2} \tan^{-1}(x-1)^{-1/2} & \text{for } x > 1 \end{cases}$$

(31)

The approach used by Yuen [9] will be adopted here. It can be shown, for the region $x < 0$, that evaluation of the leading order terms of $T_i(x, 0)$ of equation (25)

where $\xi_1 = -\beta_0$, $\xi'_1 = -\beta_1$, $\xi_2 = \beta_0/k_r$ and $\xi'_2 = \beta_1/k_r$. For regions 'away' from the leading and trailing edges of the contact region (i.e. for $P_i|x| \gg 1$ and $P_i|1-x| \gg 1$), equations (31) can be further simplified

$$T_i(x, 0) \approx \begin{cases} \frac{\exp(-2P_i|x|)}{2P_i|x|^{1/2}} \left(\frac{\xi_i}{8P_i} + \xi'_i \right) & \text{for } P_i x \ll -1 \\ \frac{1}{2} \left(\frac{\pi}{2P_i} \right)^{1/2} \xi_i x & \text{for } P_i x \gg 1 \text{ and } P_i(1-x) \gg 1 \\ \frac{\xi_i}{(2\pi P_i)^{1/2}} [x \tan^{-1}(x-1)^{-1/2} - (x-1)^{1/2}] & \text{for } P_i(x-1) \gg 1 \end{cases}$$

(32)

3.3. Temperature fields

The temperature field of body i , by substituting equation (24) into equation (1), is

$$T_i(x, y) = \frac{1}{\pi} \int_0^1 \left[\xi_i(x')^{1/2} + \frac{\xi'_i}{(x')^{1/2}} \right] e^{P_i(x-x')} \times K_0 \{ P_i [(x-x')^2 + y^2]^{1/2} \} dx'. \quad (33)$$

Approximations are now introduced to the above integral in the various regions to obtain closed-form expressions. Since the Peclet numbers are large, the temperature changes prior to the contact region are insignificant and will not be considered here.

Within the contact region, equation (33) may be written in polar coordinates

$$T_i(x, y) = \frac{\rho}{\pi} \int_0^{1/\rho} \left[\xi_i(\rho u)^{1/2} + \frac{\xi'_i}{(\rho u)^{1/2}} \right] e^{-P_i \rho(u - \cos \theta)} \times K_0 [P_i \rho(u^2 - 2u \cos \theta + 1)^{1/2}] du \quad (34)$$

where

$$x = \rho \cos \theta \quad \text{and} \quad y = \rho \sin \theta$$

such that

$$0 \leq |\theta| \leq \frac{1}{2}\pi.$$

Yuen has shown [10] that, since $P_i \rho$ is generally large and $|\theta| \ll 1$ in the region of interest, the integrand in equation (34) may be approximated, giving

$$T_i(x, y) \approx \left(\frac{1}{2\pi P_i} \right)^{1/2} \times \int_0^1 \left\{ \xi_i \rho \left(\frac{u}{1-u} \right)^{1/2} + \frac{\xi'_i}{[u(1-u)]^{1/2}} \right\} \times \exp [-2P_i \rho \sin^2(\frac{1}{2}\theta)/(1-u)] du. \quad (35)$$

The integration of the term involving ξ_i in equation

(35) is given in Appendix B, and the integration of the term involving ξ'_i follows the results of Yuen [10]. The final result is

$$T_i(x, y) = \left(\frac{2\pi}{P_i} \right)^{1/2} \{ \xi_i \rho i^2 \operatorname{erfc} [2P_i \rho \sin^2(\frac{1}{2}\theta)]^{1/2} + \frac{1}{2} \xi'_i \operatorname{erfc} [2P_i \rho \sin^2(\frac{1}{2}\theta)]^{1/2} \} \quad \text{for } 0 < x < 1. \quad (36)$$

In the region of interest, $|y| \ll x$, equation (36) can be simplified to

$$T_i(x, y) \approx \left(\frac{2\pi}{P_i} \right)^{1/2} \left[\xi_i x i^2 \operatorname{erfc} \left(\frac{P_i y^2}{2x} \right)^{1/2} + \frac{1}{2} \xi'_i \operatorname{erfc} \left(\frac{P_i y^2}{2x} \right)^{1/2} \right] \quad \text{for } 0 < x < 1. \quad (37)$$

For the region far beyond the contact such that $P_i(x-1) \gg 1$, the modified Bessel function in the integrand of equation (33) may be expanded for large argument and approximated in the region of interest ($|y| \ll x$) as illustrated in ref. [10], and equation (33) then reduces to

$$T_i(x, y) \approx \left(\frac{1}{2\pi P_i} \right)^{1/2} e^{-\eta_i} \int_0^{1/(x-1)} \left[\xi_i x \frac{u^{1/2}}{(1+u)^2} + \frac{\xi'_i}{u^{1/2}(1+u)} \right] e^{-\eta_i u} du \quad (38)$$

where

$$\eta_i = \frac{P_i y^2}{2x}. \quad (39)$$

Integration of the first term between the square brackets in equation (38) is given in Appendix C, and that for the second term follows the results of ref. [10]. The temperature distribution beyond the contact region is thus obtained

$$T_i(x, y) = \begin{cases} \frac{\xi_i}{(2\pi P_i)^{1/2}} \left\{ \pi x (\frac{1}{2} + \eta_i) \left[1 - \operatorname{erf}(\eta_i^{1/2}) \operatorname{erf} \left(\frac{\eta_i}{x-1} \right)^{1/2} \right] - (\pi \eta_i)^{1/2} x e^{-\eta_i} \operatorname{erf} \left(\frac{\eta_i}{x-1} \right)^{1/2} \right. \\ \left. - 2x e^{-\eta_i x/(x-1)} \left[\frac{(x-1)^{1/2}}{2x} + \frac{1}{2} \tan^{-1}(x-1)^{1/2} + S_1 \right] \right\} \\ + \xi'_i \left(\frac{\pi}{2P_i} \right) \left\{ \operatorname{erfc}(\eta_i^{1/2}) + \operatorname{erf}(\eta_i^{1/2}) \operatorname{erfc} \left(\frac{\eta_i}{x-1} \right)^{1/2} \right. \\ \left. - \frac{2}{\pi} e^{-\eta_i x/(x-1)} [\tan^{-1}(x-1)^{1/2} + S_2] \right\} \quad \text{for } 1 < x < 2 \\ \frac{\xi_i}{(2\pi P_i)^{1/2}} [- (x-1)^{1/2} e^{-\eta_i x/(x-1)} + x(1+2\eta_i) \tan^{-1}(x-1)^{-1/2} \\ - x e^{-\eta_i} S_3] + \xi'_i \left(\frac{2}{\pi P_i} \right)^{1/2} [\tan^{-1}(x-1)^{-1/2} - e^{-\eta_i} S_4] \quad \text{for } x > 2 \end{cases} \quad (40)$$

where S_1, S_2, S_3 and S_4 are series defined as

$$S_1 = 2 \left[\frac{2\eta_i(x-1)^{1/2}}{1.3} \right] + 3 \left[-\frac{2\eta_i(x-1)^{3/2}}{3.5} + \frac{(2\eta_i)^2(x-1)^{1/2}}{1.3.5} \right] + 4 \left[\frac{2\eta_i(x-1)^{5/2}}{5.7} - \frac{(2\eta_i)^2(x-1)^{3/2}}{3.5.7} + \frac{(2\eta_i)^3(x-1)^{1/2}}{1.3.5.7} \right] + \dots \quad (41)$$

$$S_2 = \frac{2\eta_i(x-1)^{1/2}}{1.3} + \left[-\frac{2\eta_i(x-1)^{3/2}}{3.5} + \frac{(2\eta_i)^2(x-1)^{1/2}}{1.3.5} \right] + \left[\frac{2\eta_i(x-1)^{5/2}}{5.7} - \frac{(2\eta_i)^2(x-1)^{3/2}}{3.5.7} + \frac{(2\eta_i)^3(x-1)^{1/2}}{1.3.5.7} \right] + \dots \quad (42)$$

$$S_3 = \frac{3\eta_i}{1!} \left[\frac{1}{(x-1)^{1/2}} \right] + \frac{5\eta_i^2}{2!} \left[\frac{1}{(x-1)^{3/2}} - \frac{1}{3(x-1)^{3/2}} \right] + \frac{7\eta_i^3}{3!} \left[\frac{1}{(x-1)^{5/2}} - \frac{1}{3(x-1)^{3/2}} + \frac{1}{5(x-1)^{5/2}} \right] + \dots \quad (43)$$

and

$$S_4 = \frac{\eta_i}{1!} \left[\frac{1}{(x-1)^{1/2}} \right] + \frac{\eta_i^2}{2!} \left[\frac{1}{(x-1)^{3/2}} - \frac{1}{3(x-1)^{3/2}} \right] + \frac{\eta_i^3}{3!} \left[\frac{1}{(x-1)^{5/2}} - \frac{1}{3(x-1)^{3/2}} + \frac{1}{5(x-1)^{5/2}} \right] + \dots \quad (44)$$

3.4. Thermal penetration

The maximum temperature changes (induced by the heat flux at the contact region) near the subsurface of the bodies have important implications on the thermal damage and fatigue in the solids. At a depth y below the body surface, the maximum temperature change occurs at a location $x_m(y)$, which can be determined from the solution of

$$\frac{\partial T_i}{\partial x}(x, y) = 0. \quad (45)$$

It can be shown, when the Peclet numbers are high, that the temperature change reaches a maximum at a location beyond the contact region, hence $T_i(x, y)$ is given by equation (38). On performing the differentiation and reducing the resulting expressions, it can be shown that equation (45) gives

$$\xi_i \left[-\frac{e^{-\eta_i(x-1)}}{(x-1)^{1/2}} + \frac{\pi}{2} e^{\eta_i} S_5 \right] + \frac{\xi_i'}{x} \left[(\pi\eta_i)^{1/2} \operatorname{erf} \left(\frac{\eta_i}{x-1} \right)^{1/2} - \frac{e^{-\eta_i(x-1)}}{(x-1)^{1/2}} \right] = 0 \quad (46)$$

where

$$S_5 = \begin{cases} \operatorname{erfc}(\eta_i^{1/2}) + \operatorname{erf}(\eta_i^{1/2}) \operatorname{erfc} \left(\frac{\eta_i}{x-1} \right)^{1/2} \\ -\frac{2}{\pi} e^{-\eta_i x/(x-1)} [\tan^{-1}(x-1)^{1/2} + S_2] & \text{for } 1 < x < 2 \\ \frac{2}{\pi} \tan^{-1}(x-1)^{-1/2} - \frac{2}{\pi} e^{-\eta_i} S_4 & \text{for } x > 2. \end{cases} \quad (47)$$

Once the location x_m of the maximum temperature change is determined from the non-linear equation (46), the resultant maximum temperature T_m can be obtained from equation (40).

4. DISCUSSION

4.1. Comparison with previous solutions

The leading terms of the asymptotic solutions for the contact region derived in the previous section agree with those derived from a simplified thermal analysis of two semi-infinite bodies in contact [15]: the latter solutions are identical to (i) the first term of equation (24) for the heat flux distribution to body 1, (ii) the first term of the second of equations (13) for the temperature gained by body 2 due to the internal heat generation, and (iii) the second of equations (32) and the first term of equation (37) for the surface temperature and temperature distribution in the bodies within the contact region ($0 < x < 1$), respectively. Furthermore, the temperature variations prior to and beyond the contact region, which could not be obtained from the simplified analysis of the previous work [15], have been derived in this study.

In order to establish the range of the Peclet numbers for the asymptotic solutions to be valid, they are compared with the results obtained from a numerical solution [16]. Figure 2(a) gives a comparison for the heat flux distribution to body 1 for various values of k_r and P_2 with $P_1 = 10$. It can be seen that good agreement is obtained, with P_2 reduced to as low as unity and k_r ranging from 0.1 to 10, except for regions very close to the trailing edge of the contact. Comparisons with other values of P_1 greater than 10 have also been made, and good agreement obtained in all cases. It is noted that the leading order term $f_0(x)$ varies with $x^{-1/2}$ and has a weak singularity at the leading edge of the contact. It appears that the next order term after $f_1(x)$, although not derived here, consists of a weak singularity at the trailing edge of the contact, as indicated by the numerical solution in Fig. 2(a) and observed in a previous study of a similar thermal system [9]. However, these discrepancies are not expected to produce significant errors in the temperature calculations since they span a very small region, especially when the Peclet numbers become high.

A comparison for the surface temperature dis-

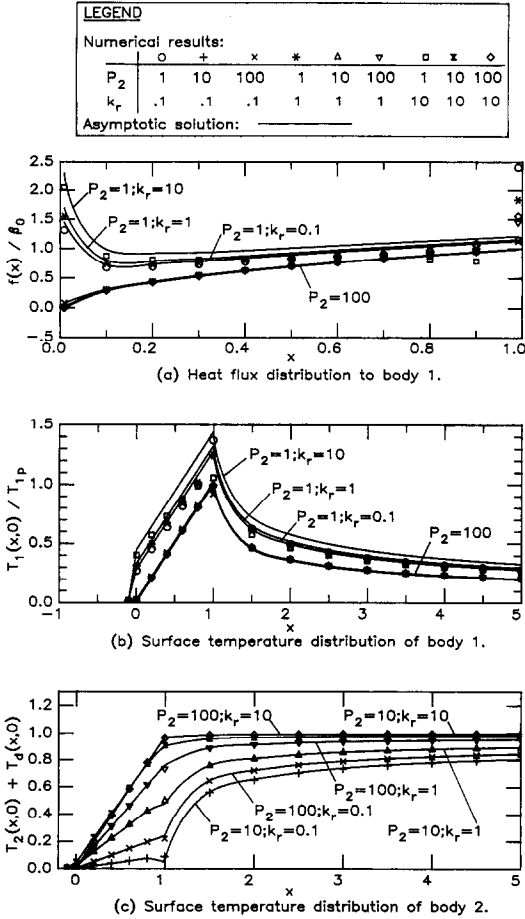


FIG. 2. Comparison between the asymptotic and numerical solutions for (a) the heat flux distribution to body 1, (b) the surface temperature distribution of body 1, and (c) the surface temperature distribution of body 2.

tributions in bodies 1 and 2 for $P_1 = 10$ are given in Figs. 2(b) and (c), respectively. In these comparisons, the temperatures have been normalized by the asymptotic peak temperature change T_{1p} for large Peclet numbers

$$T_{1p} \equiv T_1(1, 0) = \frac{1}{2} \xi_1 \left(\frac{\pi}{2P_1} \right)^{1/2} \quad (48)$$

and

$$T_{2p} \equiv T_d(1, -\infty) + T_2(1, -\infty) = 1. \quad (49)$$

It is observed that good agreement between the asymptotic and numerical solutions is obtained for the surface temperatures of bodies 1 and 2 when P_2 equals or exceeds 10. Calculations with values of P_1 exceeding 10 also produce favourable agreement, but the results are not included here in the interest of brevity.

Before a comparison between the asymptotic and numerical solutions for the temperature distribution within the bodies is made, it is necessary to examine the numerical behaviour of the series S_1, S_2, S_3 and

S_4 , which will be used to calculate the temperature distribution beyond the contact region. It is found, in agreement with a similar observation made in a previous study [10], that although each series solution was derived within its region of validity, namely, for the regions $1 < x < 2$ and $x > 2$, respectively, an overlapping region ($1.3 \leq x \leq 2$), for which both solutions are valid, exists. On examination of the numerical results, it is found that the most efficient computation would be achieved if a cross-over point of $x = 1.6$ (instead of $x = 2$) is chosen. In addition, it is observed that a 0.1% accuracy can be obtained with less than 30 terms being retained in the series if they are summed in the order written.

Figure 3 gives a comparison of the asymptotic solution with the numerical solution for body 1 for regions within and beyond the contact with $P_1 = P_2 = 10$ and $k_r = 1$. It can be seen that good agreement is obtained. Note that the temperature change varies approximately linearly with x within the contact region for positions very close to the body surfaces. With high Peclet numbers, the thermal gradients normal to the surfaces of the bodies are very high indeed. Outside the contact region, the surface temperatures again vary rapidly owing to the inward diffusion of the thermal energy driven by the high thermal gradients generated in the contact region. These are features typical of sliding solids in contact within a finite region and they have been discussed in detail in ref. [10]. Calculations have also been performed for other values of k_r, P_1 and P_2 , and the comparisons are favourable in all cases whenever P_1 and P_2 exceed 10. However, those details are omitted here in the interest of brevity.

It is concluded from the above comparisons that

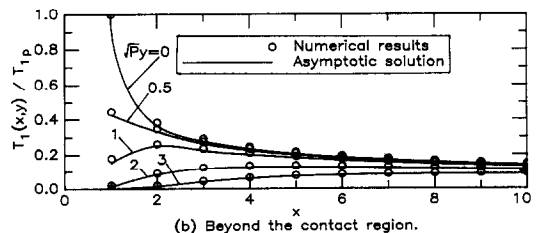
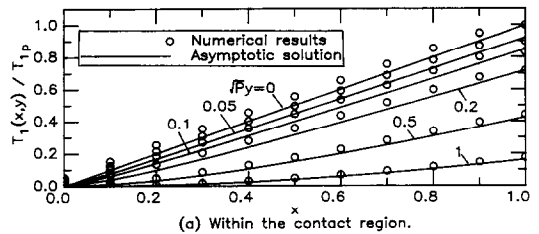


FIG. 3. Comparison between the asymptotic and numerical solutions for the temperature distribution in body 1 ($P_1 = P_2 = P, k_r = 1, P_1 = 10$ for numerical results).

the asymptotic solutions are valid when the Peclet numbers of both bodies equal or exceed 10, which covers most practical applications.

4.2. Further simplifications

In real-time process control, it is desirable to use expressions as simple, yet sufficiently accurate, as possible. While the heat flux distribution (equation (24)), the surface temperature distribution (equation (31) or (32) as appropriate), and the temperature distribution within the contact region (equation (37)) are all relatively simple expressions, the temperature distribution beyond the contact, given by equation (40), involves several infinite series. However, it has been found, during the numerical calculations in the last section, that the terms involving ξ'_i are generally insignificant and only a few terms in the remaining series need to be retained to achieve reasonable accuracy. Thus, the temperature expressions beyond the contact region may be simplified to

$$T_i(x, y) \approx \begin{cases} \xi_i \left(\frac{2\pi}{P_i}\right)^{1/2} x^2 \operatorname{erfc}(\eta_i^{1/2}) & \text{for } 1 < (x-1) < \eta_i \\ \frac{\xi_i}{(2\pi P_i)^{1/2}} \left\{ -(x-1)^{1/2} e^{-\eta_i x/(x-1)} + x e^{-\eta_i} \tan^{-1}(x-1)^{-1/2} \right. \\ \quad + 3x\eta_i e^{-\eta_i} \left[\tan^{-1}(x-1)^{-1/2} - \frac{1}{(x-1)^{1/2}} \right] \\ \quad + \frac{5}{2}x\eta_i^2 e^{-\eta_i} \left[\tan^{-1}(x-1)^{-1/2} - \frac{1}{(x-1)^{1/2}} + \frac{1}{3(x-1)^{3/2}} \right] \\ \quad \left. + \frac{7}{6}x\eta_i^3 e^{-\eta_i} \left[\tan^{-1}(x-1)^{-1/2} - \frac{1}{(x-1)^{1/2}} + \frac{1}{3(x-1)^{3/2}} - \frac{1}{5(x-1)^{5/2}} \right] \right\} & \text{for } \eta_i \geq (x-1). \end{cases} \quad (50)$$

A comparison of these approximations with the full solution of equation (40) is shown in Fig. 4(a), from which it can be seen that reasonable accuracy is achieved, especially for the region $\eta_i \geq (x-1)$.

Similarly, the non-linear equation (46) for the evaluation of the thermal penetration may be simplified to

$$\frac{\pi}{2}(x-1)^{1/2} \operatorname{erfc}(\eta_i^{1/2}) - e^{-\eta_i x/(x-1)} = 0 \quad \text{for } 0 < (x-1) < \eta_i \quad (51)$$

and

$$1 - \frac{1 + \eta_i}{3(x-1)} - e^{-\eta_i/(x-1)} = 0 \quad \text{for } \eta_i \geq (x-1). \quad (52)$$

A comparison for the locations, x_m , at which the maximum temperature change is reached for a specified depth below the body surface, determined from three different approaches is shown in Fig. 4(b). The first approach adopts a searching technique to determine x_m from the full solution of equation (40); in the second and third approaches, x_m is determined from the full equation (46) and the approximate equa-

tion (51) or (52) respectively. The corresponding maximum temperatures are shown in Fig. 4(c), with the full temperature expression of equation (40) used in the first approach and the approximated temperature expressions of equation (50) used for the other two approaches. It can be seen that, indeed, the approximations are satisfactory for all intended purposes.

4.3. Effect of heat flux distribution

It is clear from the above analysis that the temperature distribution in each sliding solid can be determined once the heat flux distribution over the contact region is known, with an extra term from the internal heat source added if appropriate. For the case where the internal heat source is absent in the body, Blok [17] stated that when the speed of the moving body is high (more precisely, when the Peclet number is high and when the heat flux distribution is largely uniform),

the maximum temperature T_p in the body (which should occur at the trailing edge of the contact on the body surface) is given by the general form

$$T_p = A \frac{q_{av}^0}{k} \left(\frac{\alpha l}{v}\right)^{1/2} \quad (53)$$

where q_{av}^0 is the average heat intensity along the contact region and A is a 'form factor' which depends on the form of the heat flux distribution over the heat input region. Blok [17] further stated that A equals $2/\pi^{1/2} \approx 1.13$ for a uniform heat flux distribution and equals 1.11 for a semi-elliptical distribution, and A would not differ very much from these values for any 'fairly smooth' heat flux distribution.

Of the numerous heat flux distributions which may be considered, those arising from the following three conditions are of practical interest when examining sliding solids which move in the same direction

- (i) where heat energy, normally frictional in nature, is generated along the contact region;
- (ii) where heat transfer across the contact region

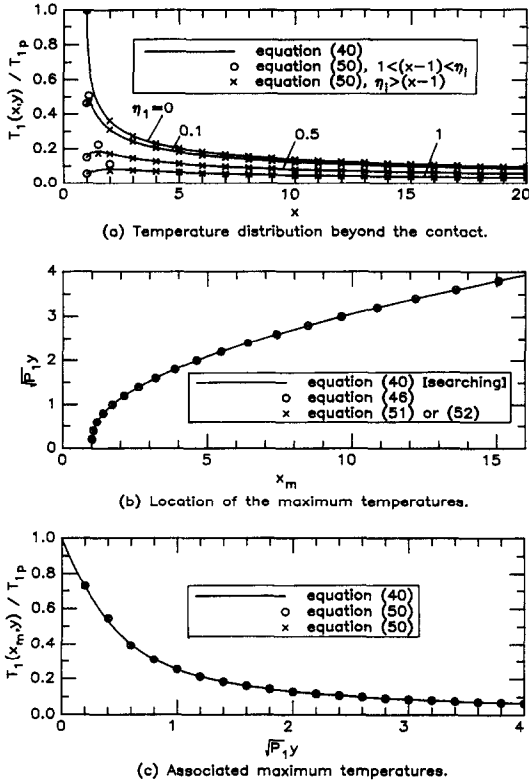


FIG. 4. Comparison of the approximated expressions with the full series solution for body 1 for (a) the temperature distribution beyond the contact region, (b) and (c) the thermal penetration.

is induced by a difference in the bulk temperatures of the solids prior to the contact; and

(iii) where heat energy, normally as a result of elastic and/or plastic deformation, is generated in one or both solids.

For ease of reference, these three cases will be called the ‘friction effect’, ‘bulk temperature difference effect’ and ‘deformation effect’, respectively. Based on an approximate analysis considering the average temperature over the contact region, Barber [18] provided an estimate of the amount of heat transferred to each body in each of these three cases. Yuen studied these with a more precise analysis and presented results for high Peclet numbers: the first two cases were discussed in refs. [9–11] and the last case discussed in this paper. In particular, the heat flux distributions to the solids for the three cases are found, in approximate terms, to be uniform, to vary with $x^{-1/2}$ and with $x^{1/2}$, respectively. It is straight-forward to show, from refs. [9–11] and the results in this paper, that the average heat fluxes transferred to a body, say, body 1, over the contact region are given by

$$(q_{av}^0)_1 = \frac{k_2 P_2^{1/2}}{k_1 P_1^{1/2} + k_2 P_2^{1/2}} q_f^0 \quad (54)$$

$$(q_{av}^0)_2 = 2 \left(\frac{2}{\pi} \right)^{1/2} \left\{ \frac{k_1 k_2 (P_1 P_2)^{1/2}}{k_1 P_1^{1/2} + k_2 P_2^{1/2}} \right\} \left(\frac{T_0}{l} \right) \quad (55)$$

$$(q_{av}^0)_3 = \frac{2}{3} \left(\frac{2}{\pi} \right)^{1/2} \frac{l k_1 P_1^{1/2}}{P_2^{1/2} (k_1 P_1^{1/2} + k_2 P_2^{1/2})} q_d^0 \quad (56)$$

where $(q_{av}^0)_i$ is the heat flux for case i , T_0 the bulk temperature difference between the two bodies, q_f^0 the rate of frictional heat generated per unit area along the contact region, and q_d^0 is the rate of heat generated per unit volume within the contact region in body 2. Further, it can be shown that the form factors for the three cases are $2/\pi^{1/2}$, $\frac{1}{2}\pi^{1/2}$ and $3\pi^{1/2}/4$, respectively. Taking the first case where the heat flux distribution is uniform as the reference, the form factors for the second and third cases are 21.5% lower and 17.8% higher, respectively. These differences are far larger than the value suggested by Blok [17] although the heat flux distributions for all cases considered are ‘fairly smooth’.

The above results are not unexpected and might be explained as follows. Since we are considering different cases with the same total heat flux applied to the body, a monotonically decreasing heat flux distribution (induced by the bulk temperature difference effect: case 2), as compared to a uniform distribution, would cause more heat to diffuse into the body due to the high heat flux during the early part of the contact, hence reducing the peak temperature reached on the body surface at the trailing edge of the contact. The reverse argument is true for a monotonically increasing heat flux distribution (induced by the deformation effect: case 3). Hence, of all possible heat flux distributions, it appears that a monotonically decreasing heat flux distribution would result in a lower overall maximum temperature change in the body. On the other hand, the thermal penetrations for all three cases are similar for locations far below the surface, as shown in Fig. 5. It can be seen from the figure that the maximum temperature reached in the body at a distance y below the body surface does not vary significantly with the heat flux distribution in the heat input region when $P^{1/2}y$ exceeds 1.

It is often desirable to obtain a quick estimate of the thermal penetration in the body. Approximate

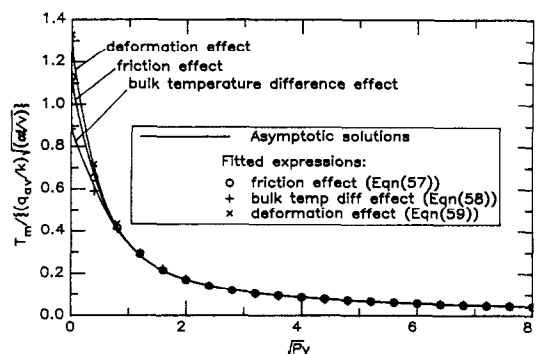


FIG. 5. Comparison between the empirically derived maximum temperatures with those from the asymptotic solutions for three heat flux distributions.

expressions may be fitted to the curves of Fig. 5; that for the friction effect has been obtained previously [11]

$$\frac{kT_m}{q_{av}^0} \left(\frac{v}{\alpha l} \right)^{1/2} = \frac{2}{\pi^{1/2}} \exp[-1.507P^{1/2}y + 0.361(P^{1/2}y)^2 - 0.0446(P^{1/2}y)^3 + 0.00208(P^{1/2}y)^4] \\ \text{for } 0 \leq P^{1/2}y \leq 8. \quad (57)$$

A suitable expression for the bulk temperature difference effect is

$$\frac{kT_m}{q_{av}^0} \left(\frac{v}{\alpha l} \right)^{1/2} = \frac{1}{2} \pi^{1/2} \\ \times \exp[-1.083P^{1/2}y + 0.1531(P^{1/2}y)^2 - 0.008(P^{1/2}y)^3] \quad \text{for } 0 \leq P^{1/2}y \leq 8 \quad (58)$$

and that for the deformation effect is

$$\frac{kT_m}{q_{av}^0} \left(\frac{v}{\alpha l} \right)^{1/2} = \frac{3\pi^{1/2}}{4} \exp[-1.714P^{1/2}y + 0.4456(P^{1/2}y)^2 - 0.0578(P^{1/2}y)^3 + 0.00278(P^{1/2}y)^4] \\ \text{for } 0 \leq P^{1/2}y \leq 8. \quad (59)$$

In equations (57)–(59), $T_m \equiv T_m(y)$ is the peak temperature (change) reached at a distance $y^0(y = y^0/l)$ below the body surface. The results from the fitted expressions are also shown in Fig. 5, from which it can be seen that excellent agreement has been obtained.

5. CONCLUSION

The heat transfer between sliding solids with internal heat sources within the contact region is examined in this paper. Both the heat flux distribution at the contact and temperature fields in the solids have been determined from an asymptotic analysis for large Peclet numbers. Comparison with a numerical solution indicates that the asymptotic solutions are valid for Peclet numbers equal to or exceeding 10. Expressions to characterize the thermal penetration into the bodies have also been derived. Simplified expressions for the temperature fields and maximum temperatures in the bodies have been obtained.

The thermal penetration obtained here has been compared with those resulting from two other heat flux distributions of practical significance. It has been found that, in general, a monotonically decreasing heat flux distribution produces a lower maximum temperature on the body surface as compared to a monotonically increasing heat flux distribution. The difference observed for the cases considered amounts to 50%. It has also been found that the thermal penetration is independent of the heat flux distribution at a sufficient depth below the body surface, namely, when $P^{1/2}y$ is greater than unity. Approximate expressions have also been obtained for a quick evaluation of the thermal penetration into the body for the three different heat flux distributions examined.

This work, together with those published previously [9–11], forms a complete analysis of the heat transfer in the roll gap of the strip rolling process, and also finds application in other similar industrial processes such as grinding and machining.

Acknowledgement—The author wishes to thank the management of BHP Steel, Sheet & Coil Products Division, for permission to publish the information contained in this paper.

REFERENCES

1. G. E. Schneider, A. B. Strong and M. M. Yovanovich, Transient thermal response of two bodies communicating through a small circular contact area, *Int. J. Heat Mass Transfer* **20**, 301–308 (1977).
2. S. S. Sadhal, Transient thermal response of two solids in contact over a circular disk, *Int. J. Heat Mass Transfer* **23**, 731–733 (1980).
3. S. S. Sadhal, Unsteady heat flow between solids with partially contacting interface, *ASME J. Heat Transfer* **103**, 32–35 (1981).
4. J. C. Jaeger, Moving sources of heat and the temperature at sliding contacts, *J. Proc. R. Soc. N.S.W.* **76**, 203–224 (1942).
5. D. N. De G. Allen, A suggested approach to finite-difference representation of differential equations, with an application to determine temperature-distributions near a sliding contact, *Q. J. Mech. Appl. Math.* **15**(1), 11–33 (1962).
6. A. Cameron, A. N. Gordon and G. T. Symm, Contact temperatures in rolling/sliding surfaces, *Proc. R. Soc.* **A286**, 45–61 (1965).
7. G. T. Symm, Surface temperatures of two rubbing bodies, *Q. J. Mech. Appl. Math.* **20**, 381–391 (1967).
8. A. G. Blahey and G. E. Schneider, The temperature field in a translating half space due to a rectangular source, *Proc. AIAA 2nd Thermophysics Conf.*, Paper No. AIAA-1987-1552 (1987).
9. W. Y. D. Yuen, A new formulation of heat transfer between two moving bodies in contact over a finite region with different bulk temperatures, *Math. Engng Industry* **1**, 1–19 (1987).
10. W. Y. D. Yuen, Temperature fields of moving bodies with different bulk temperatures in contact over a fixed region, *Math. Engng Industry* **1**, 215–234 (1987).
11. W. Y. D. Yuen, Heat conduction in sliding solids, *Int. J. Heat Mass Transfer* **31**, 637–646 (1988).
12. H. S. Carslaw and J. C. Jaeger, *Conduction of Heat in Solids* (2nd Edn), p. 267. Oxford University Press, London (1959).
13. I. S. Gradshteyn and I. Ryzhik, *Table of Integrals, Series, and Products*, pp. 339 and 714. Academic Press, New York (1980).
14. M. Abramowitz and I. A. Stegun (Eds), *Handbook of Math Functions*, pp. 300 and 505. National Bureau of Standards, US Dept of Commerce (1972).
15. W. Y. D. Yuen, On the heat transfer of a moving composite strip compressed by two rotating cylinders, *ASME J. Heat Transfer* **107**, 541–548 (1985).
16. W. Y. D. Yuen, Heat transfer analysis of sheet rolling, Ph.D. Thesis, Chapter 4. University of Wollongong, N.S.W., Australia (1984).
17. H. Blok, The flash temperature concept, *Wear* **6**, 438–494 (1963).
18. J. R. Barber, The conduction of heat from sliding solids, *Int. J. Heat Mass Transfer* **13**, 857–869 (1970).
19. A. Erdelyi, W. Magnus, F. Oberhettinger and F. G. Tricomi, *Table of Integral Transforms*, Vol. 1, pp. 208 and 220, and Vol. 2, pp. 200 and 236. McGraw-Hill (1954).

APPENDICES

Appendix A. Evaluation of integral I_a defined in equation (A.1)

Let

$$I_a = \int_0^1 (1-u)^{1/2} e^{Pu} K_0(Pu) du + \int_0^\infty (1+u)^{1/2} e^{-Pu} K_0(Pu) du \quad (A.1)$$

where $P > 0$. With $e^{Pu} K_\nu(Pu)$ expressed in terms of the Meijer's G -function, $G_{mn}^{pq}(\cdot)$ (e.g. see ref. [19]):

$$e^{Pu} K_\nu(Pu) = \frac{\cos(v\pi)}{\pi^{1/2}} G_{12}^{22}(2Pu|_{\nu, -\nu}^{1/2}) \quad (A.2)$$

both integrals in equation (A.1), with $K_0(Pu)$ replaced by the modified Bessel function of a general order, $K_\nu(Pu)$, may be evaluated [19], giving

$$\int_0^1 (1-u)^{1/2} e^{Pu} K_\nu(Pu) du = \frac{1}{2} \cos(v\pi) G_{23}^{22}(2P|_{\nu, -\nu, -3/2}^{0, 1/2}) \quad (A.3)$$

$$\int_0^\infty (1+u)^{1/2} e^{-Pu} K_\nu(Pu) du = -\frac{1}{2} G_{23}^{31}(2P|_{-3/2, \nu, -\nu}^{0, 1/2}) \quad (A.4)$$

Further, with the Meijer's G -function expressed [19] in terms of the generalized hypergeometric series, ${}_nF_m(\cdot)$, it can be shown that, after some lengthy mathematical manipulations

$$J_v \equiv \int_0^1 (1-u)^{1/2} e^{Pu} K_\nu(Pu) du + \int_0^\infty (1+u)^{1/2} e^{-Pu} K_\nu(Pu) du \quad (A.5)$$

$$= \frac{\Gamma(-2\nu)\Gamma(1+\nu)}{2(\frac{3}{2}+\nu)(\frac{1}{2}+\nu)} (2P)^\nu \times {}_2F_2(1+\nu, \frac{1}{2}+\nu; 1+2\nu, \frac{5}{2}+\nu; 2P) [\cos(v\pi) - 1] + \frac{\Gamma(2\nu)\Gamma(1-\nu)}{2(\frac{3}{2}-\nu)(\frac{1}{2}-\nu)} (2P)^\nu \times {}_2F_2(1-\nu, \frac{1}{2}-\nu; 1-2\nu, \frac{5}{2}-\nu; 2P) [\cos(v\pi) - 1] - \frac{1}{2} \Gamma(\nu + \frac{3}{2}) \Gamma(-\nu + \frac{3}{2}) \Gamma(-\frac{1}{2}) \frac{1}{(2P)^{3/2}} \times {}_2F_2(-\frac{1}{2}, -1; -\frac{1}{2}-\nu, -\frac{1}{2}+\nu; 2P) \quad (A.6)$$

where $\Gamma(\cdot)$ is the gamma function.

Since

$$\lim_{\nu \rightarrow 0} [\cos(v\pi) - 1] = -\frac{1}{2} (v\pi)^2 \quad (A.7)$$

and

$$\lim_{\nu \rightarrow 0} \Gamma(2\nu) = \frac{1}{2\nu} \quad (A.8)$$

thus

$$I_a = \lim_{\nu \rightarrow 0} J_\nu = \frac{1}{4} \left(\frac{\pi}{2P}\right)^{3/2} {}_2F_2(-\frac{1}{2}, -1; -\frac{1}{2}, -\frac{1}{2}; 2P) \quad (A.9)$$

$$= \left(\frac{\pi}{2P}\right)^{3/2} \left(\frac{1}{4} + P\right) \quad (A.10)$$

Appendix B. Evaluation of integral I_b defined in equation (B.1)

Let

$$I_b = \int_0^1 \left(\frac{u}{1-u}\right)^{1/2} e^{-p/(1-u)} du \quad (B.1)$$

where $p > 0$.

With a substitution of $w = 1-u$, I_b may be evaluated [13]

$$I_b = \int_0^1 \left(\frac{1-w}{w}\right)^{1/2} e^{-p/w} dw \quad (B.2)$$

$$= p^{-1/4} e^{-p/2} \Gamma(\frac{3}{2}) W_{-5/4, 1/4}(p) \quad (B.3)$$

Using the properties of the Whittaker function [14], it can be shown that

$$W_{-5/4, 1/4}(p) = 4\pi^{1/2} p^{1/4} e^{p/2} i^2 \operatorname{erfc}(p^{1/2}) \quad (B.4)$$

Hence

$$I_b = 2\pi^2 \operatorname{erfc}(p^{1/2}) \quad (B.5)$$

Appendix C. Evaluation of integral I_c defined in equation (C.1)

Let

$$I_c = \int_0^{1/(x-1)} \frac{u^{1/2}}{(1+u)^2} e^{-\eta u} du \quad (C.1)$$

where $\eta = \frac{1}{2} Py^2/x > 0$ and $x > 1$.

When $1 < x < 2$, the integral I_c may be evaluated between the limits from 0 to ∞ , and then from $(x-1)^{-1}$ to ∞ . Thus

$$I_c = I_{c1} - I_{c2} \quad (C.2)$$

where

$$I_{c1} = \int_0^\infty \frac{u^{1/2}}{(1+u)^2} e^{-\eta u} du \quad (C.3)$$

$$= -(\pi\eta)^{1/2} + (\frac{1}{2} + \eta)\pi e^\eta \operatorname{erfc}(\eta^{1/2}) \quad (C.4)$$

and

$$I_{c2} = \int_{1/(x-1)}^\infty \frac{u^{1/2}}{(1+u)^2} e^{-\eta u} du \quad (C.5)$$

The term $(1+u)^{-2}$ in I_{c2} may be expanded for $u > 1$ (since $1 < x < 2$) and the resultant series integrated, giving

$$I_{c2} = \sum_{m=0}^\infty \left\{ (-1)^m (m+1) \int_{1/(x-1)}^\infty u^{-m-3/2} e^{-\eta u} du \right\} \quad (C.6)$$

$$= \sum_{m=0}^\infty \left\{ (-1)^m (m+1) \eta^{m+1/2} \left[\Gamma(-m-\frac{1}{2}) - \gamma\left(-m-\frac{1}{2}, \frac{\eta}{x-1}\right) \right] \right\} \quad (C.7)$$

where $\gamma(\cdot)$ is the incomplete gamma function.

After lengthy manipulations and reductions

$$I_{c2} = -(\pi\eta)^{1/2} \operatorname{erf}\left(\frac{\eta}{x-1}\right)^{1/2} - \pi(\frac{1}{2} + \eta) e^\eta \operatorname{erf}(\eta^{1/2}) \operatorname{erf}\left(\frac{\eta}{x-1}\right)^{1/2} + 2e^{-\eta/(x-1)} \left\{ -\frac{(x-1)^{1/2}}{2x} - \frac{1}{2} \tan^{-1}(x-1)^{1/2} + \frac{1}{2} \sum_{m=1}^\infty \left[(m+1) \sum_{n=1}^m \left\{ (-1)^{m-n+1} \times \eta^n (x-1)^{m-n+1/2} \frac{\Gamma(m-n+\frac{1}{2})}{\Gamma(m+\frac{3}{2})} \right\} \right] \right\} \quad (C.8)$$

Combining these results, the integral I_c for the region $1 < x < 2$ is obtained

$$\begin{aligned}
 I_c = & (\frac{1}{2} + \eta)\pi e^\eta \left[1 - \operatorname{erf}(\eta^{1/2}) \operatorname{erf}\left(\frac{\eta}{x-1}\right)^{1/2} \right] \\
 & - (\pi\eta)^{1/2} \operatorname{erf}\left(\frac{\eta}{x-1}\right)^{1/2} + 2 e^{-\eta/(x-1)} \left\{ -\frac{(x-1)^{1/2}}{2x} \right. \\
 & - \frac{1}{2} \tan^{-1}(x-1)^{1/2} + \frac{1}{2} \sum_{m=1}^{\infty} \left[(m+1) \right. \\
 & \left. \left. \times \sum_{n=1}^m \left\{ (-1)^{m-n+1} \eta^n (x-1)^{m-n+1/2} \frac{\Gamma(m-n+\frac{1}{2})}{\Gamma(m+\frac{3}{2})} \right\} \right] \right\}. \tag{C.9}
 \end{aligned}$$

For the region $x > 2$, the exponential term in the integral

I_c may be expanded, giving

$$I_c = \sum_{m=0}^{\infty} \left\{ (-1)^m \int_0^{1/(x-1)} \frac{\eta^m u^{m+1/2}}{m!(1+u)^2} du \right\}. \tag{C.10}$$

The above integral can be integrated. The result is, after some manipulations and reductions

$$\begin{aligned}
 I_c = & -\frac{(x-1)^{1/2}}{x} e^{-\eta/(x-1)} + (1+2\eta) e^\eta \tan^{-1}(x-1)^{-1/2} \\
 & - \sum_{m=1}^{\infty} \left\{ (2m+1) \frac{\eta^m}{m!} \sum_{n=1}^m \left[\frac{(-1)^{n+1}}{(2n-1)(x-1)^{n-1/2}} \right] \right\}. \tag{C.11}
 \end{aligned}$$

When the series of equations (C.9) and (C.11) are written out, the results of equation (40) are readily obtained.